Correlation between Copper Precipitation and Grown-In Oxygen Precipitates in 300 mm Czochralski Silicon Wafer

P. Dong, X.Y. Ma* and D. Yang

State Key Laboratory of Silicon Materials and Department of Material Science and Engineering

Zhejiang University, Hangzhou 310027, China

The behaviors of copper (Cu) precipitation along the radial direction of the 300 mm Czochralski grown silicon wafer have been investigated. It is found that the density of Cu precipitates decreases from the center to edge of the silicon wafer. Moreover, it is revealed that the density of grown-in oxygen precipitates also decreases along the radial direction as mentioned above. Therefore, it is apparent that the Cu precipitate density is positively correlative to the grown-in oxygen precipitate density. This is due to that the grown-in oxygen precipitates can serve as the heterogeneous nucleation centers for Cu precipitation. It is suggested that the Cu decoration in combination with preferential etching can be used to indirectly evaluate the radial distribution of grown-in oxygen precipitates in the silicon wafers.

1. Introduction

With the feature size of integrated circuits entering into the nanometer scale, the control of grown-in defects in Czochralski (CZ) silicon has become a matter of significant technology issue. The grown-in oxygen precipitates exert substantial influence on oxygen precipitation and its related internal gettering (IG) capability [1]. It has been recently reported that the IG efficiencies are remarkably different along the axial direction of wafer, due to the different densities and sizes of grown-in oxygen precipitates [2]. Generally, the grown-in oxygen precipitates are too small to be observed by the common light-scattering and etching techniques. Even for transmission electron microscopy (TEM), it is generally appropriate for revealing the grown-in defects in size larger than 20 nm [3].

Kissinger et al. [4, 5] have developed a method to obtain the grown-in oxygen precipitate density spectra of silicon wafers, which show the density of grown-in oxygen precipitates versus the corresponding stability temperature. In this method, the ramping annealing procedures enable the grown-in oxygen precipitates at different stability temperatures to grow into larger sizes, which exceeds the detection limit of the common light-scattering and etching techniques. Following that, the oxygen precipitate density spectra are obtained by calculating the difference between the oxygen precipitate densities arisen from two successive starting temperatures of the ramping annealing.

It is well known that the grown-in oxygen precipitates can serve as as the heterogeneous nucleation sites for

copper (Cu) precipitation [6]. In this work, we have investigated the correlation between Cu precipitation and grown-in oxygen precipitates along the radial direction in a 300 mm CZ silicon wafer. It is found that the tendency of radial Cu precipitate distribution correlates well with that of the radial grown-in oxygen precipitate density spectra. Therefore, it is proposed that the Cu decoration in combination with preferential etching can be used to indirectly reflect the grown-in oxygen precipitate distribution in a silicon wafer.

2. Experiment

One 300 mm diameter boron-doped $\langle 100 \rangle$-oriented CZ silicon polished wafer with a resistivity about 10 Ωcm was utilized. The crystal growth of 300 mm CZ silicon ingot was performed on a Keyex MCZ 150 crystal puller equipped with a cusp magnetic field. Appropriate hot zone and pulling rate profile were adopted to enable the silicon crystal to be of vacancy-type defect. The interstitial oxygen concentration ([O_i]) of the wafer was $(1.04 \pm 0.03) \times 10^{18}$ cm^{-3}, measured by a Bruker IFS 66v/s Fourier transformation infrared spectrometer (FTIR) with a calibration coefficient of 3.14×10^{17} cm^{-2}. The silicon wafer was divided into five regions along the radial direction, as schematically shown in Fig. 1.

Specimens with size of 2×2 cm^2 were taken from the five regions, labeled as S1, S2, S3, S4, and S5, respectively. It should be mentioned that several specimens were taken in each region for different treatments. To investigate Cu precipitation, the specimens from the five regions were firstly dipped into 1 mol/l CuCl$_2$ solution for 20 min. After drying, they were annealed at 1000 °C for 3 min and then cooled down with a rate of ≈ 30 °C/s. It should be mentioned that the duration of 3 min definitely enabled the interstitial Cu (Cu$_i$) atoms to diffuse throughout the whole wafer [7, 8]. Such annealed specimens were chemically polished for 1 min using mixed

—————

*corresponding author; e-mail: mxyoung@zju.edu.cn
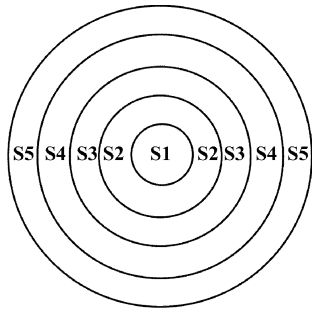
Fig. 1. Schematic diagram for one 300 mm CZ silicon wafer divided into five regions.

solution of HNO_3 and HF with a volume ratio of 3:1 in order to remove the residual Cu film on the surface. Cu precipitates were delineated by preferential etching in Secco etchant [$K_2Cr_2O_7$ (0.15 mol/L): HF (49%) = 1:2] for 3 min, in combination with the observation using an Olympus MX50 optical microscope (OM) equipped with a CCD camera.

Moreover, to clarify the influence of grown-in oxygen precipitates on Cu precipitation in the specimens taken from different regions in the silicon wafer, the S1 (in the center region) and S5 (in the edge region) specimens received a prior rapid thermal processing (RTP) at 1250 °C for 60 s in argon ambient, with an average cooling rate of 3 °C/s. It should be mentioned that the RTP with such a small cooling rate will not inject considerable amount of vacancies in silicon, which will not have significant effect on Cu precipitation. Subsequently, the two specimens received the above-mentioned thermal treatment for Cu precipitation.

In order to obtain the density of grown-in oxygen precipitates, four specimens taken from each region received 8 h anneal at 1150 °C ramped up from 500, 600, 700 and 800 °C, respectively, with a rate of 1 °C/min. Such annealing schemes used the same ramping rate as those described elsewhere [4]. At the ramping rate of 1 °C/min, the growth rate of oxygen precipitates is comparable to the increase of the critical radius of oxygen precipitate nuclei [4, 5]. A higher ramping rate, such as 3.3 °C/min or above, results in a faster increase of the critical radius of oxygen precipitate nuclei during annealing, and thus causes the shrink of smaller oxygen precipitate nuclei [5]. The densities of oxygen precipitates in such annealed specimens were measured by a Semilab SIRM-300 scanning infrared microscope (SIRM). According to the methodology presented by Kissinger et al. [4], the defect density spectra were obtained by calculating the difference between the oxygen precipitate densities arisen from two successive starting temperatures of the ramping annealing as mentioned above. That is, the oxygen precipitate density spectra can be calculated in terms of the following expressions:

$$n_{grow}(500\,°C) = n_{OP}(500\,°C) - n_{OP}(600\,°C),$$

$$n_{grow}(600\,°C) = n_{OP}(600\,°C) - n_{OP}(700\,°C),$$

$$n_{grow}(700\,°C) = n_{OP}(700\,°C) - n_{OP}(800\,°C), \qquad (1)$$

where $n_{OP}(500\,°C)$, $n_{OP}(600\,°C)$, $n_{OP}(700\,°C)$, and $n_{OP}(800\,°C)$ are the SIRM measured oxygen precipitate densities after the ramping anneals starting from 500, 600, 700, and 800 °C, respectively. Thus, the calculated $n_{grow}(500\,°C)$ is the density of oxygen precipitate nuclei, which is stable at 500 °C and shrinks at the temperatures of 600 °C and higher.

3. Results and discussion

Figure 2 shows the OM images of Cu precipitates in the specimens S1–5 taken along the radial direction of the 300 mm CZ silicon wafer. In all specimens the Cu precipitates are delineated as the aggregated or individual rods. Moreover, the density and size of Cu precipitates decrease from S1 to S5, namely, from the center to edge of the silicon wafer.
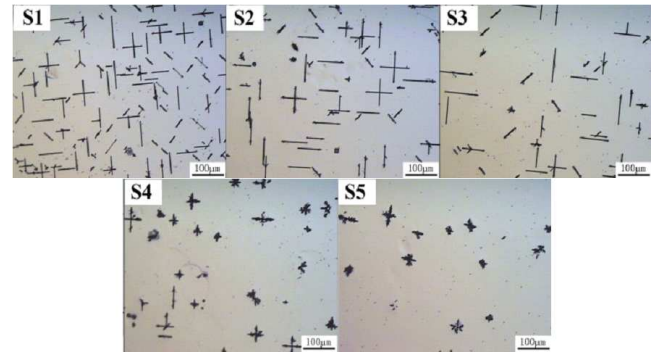
Fig. 2. OM images of the Cu precipitates formed in S1–5 specimens taken along the radial direction of wafer, which were subjected to annealing at 1000 °C for 3 min followed with an average cooling rate of 30 °C/s.

Figure 3 shows the OM images of Cu precipitates in the specimens S1 and S5, which received the prior RTP at 1250 °C for 60 s. It should be mentioned that such a RTP with quite small cooling rate (3 °C/s) did not induce considerable vacancies in the specimens S1 and S5, which had nearly no influence on the Cu precipitation during the subsequent annealing. As can be seen from Fig. 3, the morphologies and densities of Cu precipitates in the two specimens exhibit no essential difference. The Cu precipitates are delineated as the etching pits, which are based on the homogeneous nucleation driven by the supersaturation of Cu_i atoms [9, 10]. Moreover, it has been proved that the RTP at 1250 °C can substantially dissolve the grown-in oxygen precipitates [6]. Therefore, the effect of grown-in oxygen precipitates on Cu precipitation in the two specimens S1 and S5 can be excluded. Based on the results as revealed in Figs. 2 and 3, it is derived that the difference in Cu precipitate density from the center to edge of the silicon wafer is pertaining to the radial distribution of grown-in oxygen precipitates.
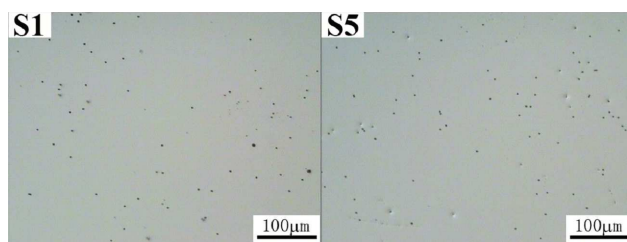
Fig. 3. OM images of Cu precipitates in the specimen S1 and S5, with the prior RTP at 1250 °C for 60 s with an average cooling rate of 3 °C/s in Ar, followed by the annealing for Cu precipitation at 1000 °C for 3 min in Ar with cooling rate of 30 °C/s.

Figure 4 shows the grown-in oxygen precipitate density spectra for S1–5 specimens taken from different regions of the silicon wafer. Herein, the densities of the grown-in oxygen precipitates with stability temperatures of 500, 600, and 700 °C, respectively, are given. It can be seen that the densities of grown-in oxygen precipitates decrease from S1 to S5, i.e. from the center to the edge of the silicon wafer. According to Voronkov et al.'s theory [11–13], it is known that during the crystal growth the number of vacancies incorporated into the silicon crystal decreases from the center to the edge along the radial direction.
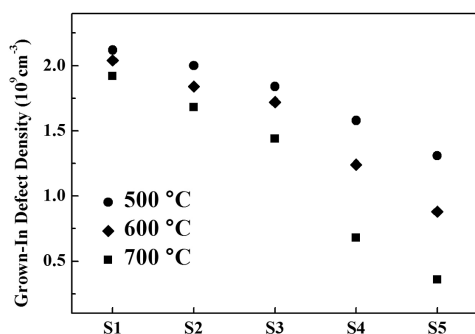
Fig. 4. Grown-in oxygen precipitates density spectra for the S1–5 specimens taken along the radial direction of 300 mm silicon wafer.

On the other hand, the post-growth cooling rate increases from the edge to the center of the silicon ingot. Therefore, in the case of vacancy-type crystal growth, it is believed that the vacancy-assisted oxygen precipitation during the crystal growth becomes ever-stronger from the edge to the center of silicon ingot. Concerning a silicon wafer, it is manifested that the density and size of grown-in oxygen precipitates decrease from the center to the edge, as shown in Fig. 4. In view of the results of Figs. 2 and 4, we believe that the Cu precipitate density is positively correlative to the grown-in oxygen precipitate density. This is due to that the grown-in oxygen precipitates can serve as the heterogeneous nucleation centers for Cu precipitation.

Generally, the stress around the larger grown-in oxygen precipitates is larger than that around the smaller grown-in oxygen precipitates. Therefore, the nucleation energy barrier for Cu precipitation is lower at the larger grown-in oxygen precipitates than that at the smaller grown-in oxygen precipitates. Thus, the Cu_i atoms are incline to precipitate on the larger grown-in oxygen precipitates. Like the case of oxygen precipitation, Cu precipitation is usually accompanied with ejection of interstitial silicon (Si_i) atoms due to the volume expansion. In certain regions, the supersaturated Si_i atoms may aggregate into dislocations [14]. Then, Cu precipitate colonies form through the repeated aggregation of Cu_i atoms on the climbing dislocations [15, 16]. In this context, the Cu precipitates are delineated as aggregated and individual rods as shown in Fig. 2. As mentioned above, Cu precipitation occurred during the cooling of annealing at 1000 °C for 3 min. In such a short thermal cycle, most of the grown-in oxygen precipitates can survive. Obviously, the radial distribution of the survived grown-in oxygen precipitates has the same tendency as that shown in Fig. 4. In consequence, the radial distribution of Cu precipitates should be essentially affected by the grown-in oxygen precipitates, that is, both the density and size of Cu precipitates decrease from the center to the edge of the silicon wafer.

4. Conclusion

In summary, the behaviors of Cu precipitation along the radial direction of the 300 mm CZ silicon wafer have been investigated. It is found that the grown-in oxygen precipitates can serve as the heterogeneous nucleation centers for Cu precipitation, leading to rod-like Cu precipitates. In the case of using the prior RTP at 1250 °C to dissolve the grown-in oxygen precipitates, the Cu precipitates based on the homogeneous nucleation driven by the supersaturation of Cu_i atoms are delineated as the etching pits. Moreover, it is revealed that both the densities of grown-in oxygen precipitate and Cu precipitates decrease from the center to the edge along the radial direction of the silicon wafer. Therefore, the Cu precipitate density is positively correlated to the grown-in oxygen precipitate density. In a way, we can use Cu decoration in combination with preferential etching to indirectly reflect the radial distribution of grown-in oxygen precipitate across a silicon wafer.

References

[1] Y.H. Zeng, X.Y. Ma, J.H. Chen, W.J. Song, W.Y. Wang, L.F. Gong, D.X. Tian, D.R. Yang, *J. Appl. Phys.* **111**, 033520 (2012).

[2] I. Lee, U. Paik, J. Park, *J. Cryst. Growth* **365**, 6 (2013).

[3] B.S. Moon, B.C. Sim, J.G. Park, *Jpn. J. Appl. Phys.* **49**, 121301 (2010).

[4] G. Kissinger, D. Graf, U. Lambert, H. Richter, *J. Electrochem. Soc.* **144**, 1447 (1997).

[5] G. Kissinger, T. Grabolla, G. Morgenstern, H. Richter, D. Graf, J. Vanhellemont, U. Lambert, W. von Ammon, *J. Electrochem. Soc.* **146**, 1971 (1999).

[6] W.Y. Wang, D.R. Yang, X.Y. Ma, D.L. Que, *J. Appl. Phys.* **104**, 013508 (2008).

[7] A.A. Istratov, E.R. Weber, *J. Electrochem. Soc.* **149**, G21 (2002).

[8] R.N. Hall, J.H. Racette, *J. Appl. Phys.* **35**, 379 (1964).

[9] Z.Q. Xi, D.R. Yang, J. Xu, Y.K. Ji, D.L. Que, H.J. Moeller, *Appl. Phys. Lett.* **83**, 3048 (2003).

[10] Z.Q. Xi, J. Chen, D.R. Yang, A. Lawerenz, H.J. Moeller, *J. Appl. Phys.* **97**, 094909 (2005).

[11] V.V. Voronkov, *J. Cryst. Growth* **59**, 625 (1982).

[12] V.V. Voronkov, R. Falster, *J. Cryst. Growth* **204**, 462 (1999).

[13] R. Falster, V.V. Voronkov, *Phys. Status Solidi B-Basic Res.* **222**, 219 (2000).

[14] F. Cristiano, J. Grisolia, B. Colombeau, M. Omri, B. de Mauduit, A. Claverie, L.F. Giles, N.E.B. Cowern, *J. Appl. Phys.* **87**, 8420 (2000).

[15] E. Nes, J. Washburn, *J. Appl. Phys.* **42**, 3562 (1971).

[16] E. Nes, J.K. Solberg, *J. Appl. Phys.* **44**, 486 (1973).